Electron scattering from 2-methyl–1,3-butadiene, C_5H_8, molecules: Role of methylation

Czesław Szmytkowski,* Sylwia Stefanowska, Mateusz Zawadzki, Elżbieta Ptasińska-Denga, and Paweł Możejko
Atomic Physics Division, Department of Atomic, Molecular, and Optical Physics,
Faculty of Applied Physics and Mathematics, Gdańsk University of Technology,
ul. G. Narutowicza 11/12, 80-233 Gdańsk, Poland
(Received 9 June 2016; published 13 October 2016)

We report cross-section results from experimental and theoretical investigations into electron collisions with the 2-methyl–1,3-butadiene [C_5H_8] molecule. The current results are compared with our previous results for the 1,3-butadiene [C_4H_6] molecule, a structural homologue of 2-methyl–1,3-butadiene, to investigate how the methylation (the substitution of hydrogen atom by a methyl group) affects the shape and/or magnitude of the total cross sections (TCSs). Both experimental TCS energy dependencies have certain features in common: the Ramsauer–Townsend-like minimum located within 1.4–1.6 eV; the resonant maximum centered at 3.4 eV for the 2-methyl–1,3-butadiene molecule and at 3.2 eV for 1,3-butadiene; a weak shoulder in the vicinity of 7 eV; and the pronounced broad enhancement peaking around 8.5 eV for 2-methyl–1,3-butadiene and near 9.5 eV for 1,3-butadiene. The magnitude of the TCS for 2-methyl–1,3-butadiene appears to be higher than that for 1,3-butadiene over the whole investigated energy range. Closer analysis of data shows that the TCS for 2-methyl–1,3-butadiene can be reasonably reproduced by the sum of TCSs for 1,3-butadiene and half of the TCS for the ethane [C_2H_6] molecule—that stays for the TCS of the methyl unit [CH_3]. That result can be extended to homologous series of methyl-substituted allenes, ethylenes, and acetylenes.

DOI: 10.1103/PhysRevA.94.042706

I. INTRODUCTION

Electron-molecule interactions in collisions proved to be very important processes in nature and many areas of science and new technology [1]. A thorough understanding and accurate modeling of elementary electron-assisted processes in various media; namely, effects of ionizing radiation in living cells [2–4], processes in the atmosphere [5], controlling plasma-enhanced reactors [6], technology of electron-beam-induced deposition (EBID) [7–9], just to name a few, requires comprehensive sets of respective measurables (the electron scattering cross sections, reaction rates, and electron transport parameters) for various scattering channels. For the bulk of biologically and practically important hydrocarbons, which are usually rather complex compounds, the electron-scattering data are not available due to experimental and/or computational difficulties. At the deficiency of direct results for complex hydrocarbons, the input data for the simulation of electron-induced events in media containing such compounds can be estimated by using results available for their prototypes, subunits, or based on regularities found in results for other targets. Search for such regularities requires investigations of how the measured scattering quantities change together with the physico-chemical parameters of molecules, e.g., with the substitution of functional groups. These studies could also provide some insight into the role of the molecular structure in the scattering dynamics.

The main aim of this work is to examine how the replacement of the hydrogen atom in a molecule with the methyl group [CH_3] is reflected in the shape and magnitude of the total cross section (TCS). For that reason we first measured and computed the cross sections for the electron scattering from the 2-methyl–1,3-butadiene [$H_2C{=}C(CH_3)HC{=}CH_2$] molecule. Then, we compared the current experimental absolute TCS results for the 2-methyl–1,3-butadiene molecule to our previous TCS data [10] for its structural homologue 1,3-butadiene [$H_2C{=}CHHC{=}CH_2$] to search for differences and/or similarities in TCSs associated with methylation; the schematic geometry of these compounds, with conjugated double C=C bonds, is depicted in Fig. 1.

Finally, we prove that the TCS for the 2-methyl–1,3-butadiene molecule can be reasonably approximated by the sum of TCSs for its two "constituents": 1,3-butadiene and the methyl unit; the TCS for the CH_3 was taken as half of TCS for the ethane molecule (from Ref. [11]). We also found that such additivity procedure is applicable for series of methylated derivatives of allene, ethylene, and acetylene. That finding may be very useful for the estimation of cross sections for more complex, methylated targets, for which measurements and/or calculations are at present not possible.

2-methyl–1,3-butadiene (isoprene) is one of the most abundant among atmospheric trace compounds, to which human exposure is unavoidable. It occurs in the environment as emissions from vegetation and as a by-product in a large-scale petrochemical industry. Apart from its important role in Earth's atmosphere [12], 2-methyl–1,3-butadiene constitutes the building block of natural rubber, terpenes, and important biological compounds such as chlorophyll or vitamin A. Because 2-methyl–1,3-butadiene is also produced endogenously in humans, a level of this hydrocarbon in exhaled breath is considered as a noninvasive biomarker in medicine [13]. Despite the biological and industrial importance of the 2-methyl–1,3-butadiene molecule, the electron-scattering studies for this compound are exceptionally scarce and fragmentary. The electron-impact ionization technique was used to determine the ionization potential for the 2-methyl–1,3-butadiene molecule [14] and to study on the concentration of this compound in the tropical forest [15]. Electron energy-loss spectroscopy was employed to derive photoabsorption cross

*czsz@mif.pg.gda.pl

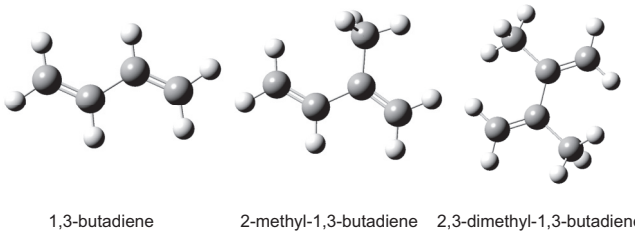

FIG. 1. Geometry of the 1,3-butadiene molecule and its methylated derivatives: 2-methyl–1,3-butadiene and 2,3-dimethyl–1,3-butadiene.

sections [16]. We also noticed that geometrical parameters of the 2-methyl–1,3-butadiene molecule have been investigated by using the electron-diffraction technique [17].

II. MEASUREMENTS

The absolute TCSs for the electron scattering from 2-methyl–1,3-butadiene were determined by using the linear electron-transmission method over an incident energy range from 0.6 to 300 eV. The method is based on measurements of the projectile electron-beam intensity attenuation while transmitted through the reaction volume filled with the target molecules. The apparatus and measurement procedure used in this work have been extensively employed in our previous TCS experiments and described in detail elsewhere [18], so only a brief summary is repeated here. The beam of electrons, generated by the thermionic emission from a hairpin thoriated-tungsten filament, is formed by an electron-transport system composed of an electron gun coupled to an energy-dispersing 127° electrostatic deflector and an assembly of electrostatic lenses. Electron optics of the spectrometer is housed in a vacuum chamber evacuated to a base pressure of about 40 μPa. The electrons of desired energy E ($\Delta E < 0.1$ eV, full width at half maximum or FWHM) are forwarded into the reaction cell where they may interact with the target particles. The energy of the incident electron beam is established with respect to the resonant oscillatory structure visible around 2.3 eV (see, e.g., Refs. [19,20]) when the N_2 is admixtured. The electrons leaving the cell through the exit orifice enter a retarding field analyzer (RFA), which discriminates those scattered inelastically in the forward direction. The Faraday cup, following the RFA, is used for detection of the transmitted electrons. The magnetic field along the whole electron pathway in the spectrometer is reduced below 100 nT by using the system of Helmholtz coils.

In the electron-transmission method, the total cross section Q at given electron impact energy E can be obtained according to the Bougue–de Beer–Lambert (BBL) attenuation formula:

$$I_n(E) = I_0(E)\exp[-nLQ(E)].$$

Here, $I_n(E)$ and $I_0(E)$ are the measured intensities of the electron beam passing the distance L through the reaction volume in the presence or absence of the target vapor, respectively. n is the number density of the target molecules in the scattering cell; that has been derived from the ideal gas formula corrected for the thermal transpiration effect [21]

$$n = \frac{p_t}{k\sqrt{T_t T_m}},$$

where p_t means the pressure of the vapor-target in the cell as measured by a Baratron capacitance manometer, T_t is the temperature of the target cell determined by using a thermocouple, $T_m = 322\ \mathrm{K} > T_t$ is the temperature at which the manometer head is held, and k denotes the Boltzmann constant.

The target vapor is introduced into the spectrometer via a variable leak valve, alternately into the reaction cell and the outer vacuum volume, thus the pressure in the region of the electron optics is kept constant (below 0.6 mPa), independently of whether the target is present in the cell or not. The TCS measurements have been carried out at target-vapor pressures, which typically lay between 80 and 200 mPa. Under these conditions no systematic variation of the measured TCSs with the pressure is observed; thus one can assume that multiple scattering events are not significant.

The acquisition and processing of data necessary for the TCS derivation is performed under computer control. To confirm the validity of experimental procedure used, the TCSs for molecular nitrogen have been measured at some energies; agreement with the reference data [22] is very good.

The quantities in the attenuation BBL formula are taken directly in the course of experiment and therefore the TCS values reported in this work are given in absolute units, without any normalization procedure. The final TCS at given energy is derived as the weighted average of TCS values obtained in different runs. The statistical variations of TCS, estimated as one standard deviation of the weighted mean value, do not exceed 1% below 100 eV, and 2% over the remaining range of the electron-impact energies applied.

Because the conditions under which the BBL formula is valid are not strictly fulfilled in the electron-transmission experiments [23], the obtained TCS data usually systematically differ from the *true* TCS values. The comparison of TCS results obtained in different laboratories shows divergences, which even for simple compounds (e.g., CO, O_2; see Ref. [22]) often exceed the common declared uncertainties and have a systematic character.

The systematic uncertainty of our absolute TCSs for 2-methyl–1,3-butadiene, evaluated as a direct sum of all individual potential systematic uncertainties, amounts up to 11% between 0.6 and 1 eV, decreasing to 7%–9% within 1–2 eV, and to about 5%–6% between 2 and 100 eV, increasing again to 7%–8% at higher energies. The most prominent contributions to the overall TCS systematic uncertainty come from:

(i) the inability to discriminate against electrons scattered elastically through the small angles in the forward direction: The *forward-scattering effect* is a common trouble in electron-transmission experiments; it leads to an overestimation of the measured I_p intensity, and hence to systematic lowering of the measured TCS with respect to its *true* value. It also can permanently distort the shape of the TCS energy dependence, especially at low electron-impact energies [24]. Having in hand the appropriate differential cross sections (DCSs) and taking into account the geometry of the scattering and detection

TABLE I. Absolute experimental electron-scattering total cross sections (TCSs) for the 2-methyl–1,3-butadiene molecule; in units of 10^{-20} m^2.

E (eV)	TCS	E (eV)	TCS	E (eV)	TCS	E (eV)	TCS	E (eV)	TCS
0.6	53.1	1.9	38.2	4.3	55.2	12.5	63.7	80	39.8
0.7	52.7	2.0	39.4	4.6	57.1	14.5	61.9	90	38.1
0.8	51.8	2.1	40.5	5.0	60.0	16.5	60.0	100	36.3
0.9	49.1	2.2	41.2	5.5	62.4	18.5	58.8	110	34.1
0.95	46.9	2.3	42.4	6.0	64.4	21	57.6	120	32.7
1.0	44.9	2.4	43.8	6.5	65.8	23	56.3	130	31.4
1.05	44.1	2.5	45.1	7.0	66.4	26	55.4	140	29.7
1.1	42.8	2.6	46.7	7.5	67.2	28	54.9	160	26.6
1.2	41.0	2.8	49.8	8.0	68.9	30	53.5	180	24.4
1.3	38.9	3.0	53.0	8.5	69.1	35	51.7	200	22.1
1.4	37.9	3.2	55.4	9.0	68.7	40	49.6	220	20.4
1.5	37.4	3.4	56.3	9.5	68.0	45	48.2	250	17.7
1.6	37.1	3.6	56.0	10	66.9	50	46.6	300	14.8
1.7	37.2	3.8	53.9	10.5	65.9	60	44.2		
1.8	37.8	4.1	54.0	11.5	64.8	70	41.7		

regions, one can roughly estimate the portion by which the measured TCS is lowered and then correct the obtained value for this effect. Due to lack of DCS data for 2-methyl–1,3-butadiene we assumed, based on the estimates for the targets of similar physical properties, that the measured TCSs for electron scattering from 2-methyl–1,3-butadiene may be lowered by about 3%–4% at low impact energies and 4%–5% at intermediate energies. Note that the reported TCS data (see Table I) are not corrected for the forward-angle-scattering effect.

(ii) the inability to correctly determine the factor nL in the BBL formula due to the inevitable effusion of the target molecules through orifices of the scattering cell. The effusion leads to inhomogeneous target distribution in the cell and to the presence of the target particles also outside the reaction cell, close to the apertures. Following the calculations from Ref. [25], the TCS uncertainty related to the nL was estimated to be about 1.5%–2%.

(iii) the drift in energy up to 0.1 eV, noticed during the long-term experiment, due to the contamination of electron optics elements by target molecules. That effect may somewhat distort the TCS structures at low impact energies.

Possible systematic errors, related to other quantities taken in the present experiment, are estimated to be less than 1% each. The sample (99+%) of 2-methyl–1,3-butadiene from Sigma-Aldrich was distilled by freeze-pump-thaw cycles before use.

III. NUMERICAL CALCULATIONS

The main goal of the present calculations is to estimate the total electron-scattering cross section for the 2-methyl–1,3-butadiene and 1,3-butadiene molecules at high impact energies, which lie beyond the upper accessible limit in our experiments. For this purpose we have performed calculations of cross sections for the elastic electron-scattering (ECS) and for the electron-induced ionization (ICS); the sum of ECS and ICS approximates the total scattering cross section.

Elastic cross sections for the electron collision with the studied targets have been calculated by using the additivity rule (AR) [26], while ionization cross sections have been obtained within the binary-encounter-Bethe (BEB) [27] formalism.

In the AR approximation the integral ECS for the electron scattering from a molecule is given by

$$\sigma^{\mathrm{el}}(E) = \frac{4\pi}{k}\sum_{i=1}^{N}\mathrm{Im}\, f_i(\theta = 0,k) = \sum_{i=1}^{N}\sigma_i^{\mathrm{A}}(E),$$

where $f_i(\theta,k)$ is the scattering amplitude due to the ith atom of the target molecule, θ is the scattering angle, while E and $k = \sqrt{2E}$ stand for the energy and wave number of the incident electron, respectively. The ECS for the ith atomic constituent of the molecule, $\sigma_i^{\mathrm{A}}(E)$, has been derived according to

$$\sigma^{\mathrm{A}} = \frac{4\pi}{k^2}\left(\sum_{l=0}^{l_{\max}}(2l+1)\sin^2\delta_l + \sum_{l=l_{\max}+1}^{\infty}(2l+1)\sin^2\delta_l^{(\mathrm{B})}\right).$$

To obtain phase shifts δ_l, a partial-wave analysis has been employed and the radial Schrödinger equation

$$\left[\frac{d^2}{dr^2} - \frac{l(l+1)}{r^2} - 2[V_{\mathrm{stat}}(r) + V_{\mathrm{polar}}(r)] + k^2\right]u_l(r) = 0$$

has been solved numerically under the boundary conditions

$$u_l(0) = 0, \quad u_l(r) \overset{r\to\infty}{\longrightarrow} A_l\hat{j}_l(kr) - B_l\hat{n}_l(kr),$$

where $\hat{j}_l(kr)$ and $\hat{n}_l(kr)$ are the Riccati–Bessel and Riccati–Neumann functions, respectively.

Our previous intermediate-energy studies (see, e.g., Ref. [28]) have shown that the AR method, with only the static and polarization parts of the electron-target interaction, can reproduce experimental elastic integral cross sections quite satisfactorily. Therefore, in the present calculations the electron-atom interaction has been represented just by sum of the static, $V_{\mathrm{stat}}(r)$, [29] and polarization, $V_{\mathrm{polar}}(r)$, [30]

potentials, which are given by following expressions:

$$V_{\text{stat}}(r) = -\frac{Z}{r}\sum_{m=1}^{3}\gamma_m \exp(-\beta_m r),$$

where Z is the nuclear charge of the atom, γ_m and β_m are parameters obtained by fitting to the numerical Dirac–Hartree-Fock-Slater screening function [29]:

$$V_{\text{polar}}(r) = \begin{cases} v(r), & r \leqslant r_c \\ -\alpha/2r^4, & r > r_c, \end{cases}$$

where $v(r)$ is the free-electron-gas correlation energy [31], α means the static electric-dipole polarizability of atom, and r_c is the first crossing point of the $v(r)$ and $-\alpha/2r^4$ curves [32].

The phase shifts δ_l are connected with the asymptotic form of the wave function, $u_l(r)$, by

$$\tan\delta_l = \frac{B_l}{A_l}.$$

In the present calculations the exact phase shifts have been calculated for l up to $l_{\max} = 50$ while those remaining, $\delta_l^{(\text{B})}$, have been included through the Born approximation.

Within the binary-encounter-Bethe model the electron-impact ionization cross section for a given molecular orbital is expressed by formula [27]

$$\sigma^{\text{BEB}} = \frac{S}{\epsilon + u + 1}\left[\frac{\ln\epsilon}{2}\left(1 - \frac{1}{\epsilon^2}\right) + 1 - \frac{1}{\epsilon} - \frac{\ln\epsilon}{\epsilon + 1}\right],$$

where $S = 4\pi a_0^2 N R^2/B^2$ ($a_0 = 0.5292$ Å, $R = 13.61$ eV), $u = U/B$, $\epsilon = E/B$, and E is the energy of the impinging electron.

The total cross section σ^{ion} for the electron-impact ionization of molecule can be obtained as the sum of ionization cross sections for all molecular orbitals, i.e.,

$$\sigma^{\text{ion}} = \sum_{j=1}^{n_{\text{MO}}}\sigma_j^{\text{BEB}},$$

where n_{MO} is the number of molecular orbitals.

The advantage of the BEB model is that all quantities necessary to calculate ICS have the exact physical meaning and can be calculated or evaluated with standard quantum chemistry methods. In the present work, the electron binding energy B, the kinetic energy of the orbital, U, and the orbital occupation number N, have been calculated for the geometrically optimized 2-methyl–1,3-butadiene and 1,3-butadiene molecules with the Hartree–Fock method by using the GAUSSIAN code [33], and the standard Gaussian 6-31G++ basis set. Because ionization energies obtained by using Koopmans' theorem differ usually from the experimental values, we also performed outer-valence Green's function calculations of correlated electron affinities and ionization potentials [34–37] by using the same GAUSSIAN code.

Finally, the total electron-scattering cross section is obtained as the sum, ECS + ICS, of the elastic (ECS) and ionization (ICS) cross sections calculated for the investigated targets. Based on our previous studies [38–44], we can state that, by using that rather simple approximation, it is possible to estimate the total cross section for the electron–molecule scattering quite satisfactorily.

IV. RESULTS AND DISCUSSION

In this section we first present our experimental and theoretical results for electron scattering from the 2-methyl–1,3-butadiene molecule. Observed TCS structures are explained based on data for molecules of similar structure. Then, to examine how the methylation of the molecule reflects in the TCS energy dependence, the TCS data for 2-methyl–1,3-butadiene and its homologue 1,3-butadiene (from Ref. [10]) are compared. Differences and similarities of compared TCS energy curves are pointed out and discussed. Next, we show that the TCS energy dependence for the 2-methyl–1,3-butadiene molecule can be reasonably reproduced by sum of the TCS for 1,3-butadiene and the TCS for methyl unit (estimated as half of the TCS for ethane). To check if that procedure is applicable to other targets we extend our examination to some series of methyl-substituted compounds. Finally, we used a similar procedure to predict electron-scattering TCS energy dependencies for a few methylated targets.

A. 2-methyl–1,3-butadiene, $H_2C{=}C(CH_3)HC{=}CH_2$

Figure 2 shows the energy dependence of the present experimental TCS together with the computed ECS and ICS, and their sum, ECS + ICS. No other experimental or theoretical electron-scattering TCS data for 2-methyl–1,3-butadiene have been found in the literature for comparison. As the reported absolute scattering cross sections can serve as an input set when modeling and simulating physicochemical effects induced by electrons traversing through matter, numerical data are also listed in Tables I and II.

The measured TCS energy dependence for the electron—2-methyl–1,3-butadiene scattering, depicted in Fig. 2, is dominated with two pronounced enhancements separated with

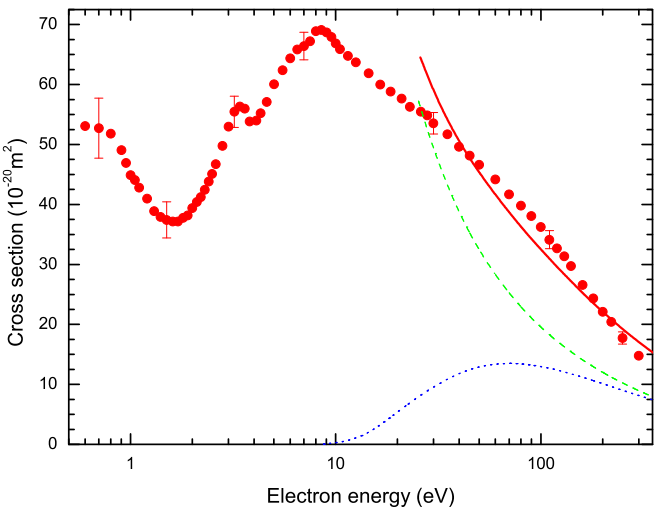

FIG. 2. Cross sections for electron scattering from the 2-methyl–1,3-butadiene molecule. Experimental data shown by full (red) circles, TCS (present work). Error bars correspond to overall (systematic plus statistical) experimental uncertainties at selected points. Theoretical data: dashed (green) line shows ECS calculated with the AR approach (present work), while dotted (blue) line shows ICS in the BEB approximation (present work). Solid (red) line shows ECS + ICS (present work).

TABLE II. Ionization (ICS) and elastic (ECS) cross sections calculated for electron impact on 2-methyl–1,3-butadiene molecules; in units of 10^{-20} m^2.

E (eV)	ICS	E (eV)	ICS	ECS	E (eV)	ICS	ECS	E (eV)	ICS	ECS
8.638	0									
9	0.0712	25	7.84	57.94	85	13.33		350	7.39	7.93
10	0.279	30	9.61	49.25	90	13.23	21.04	400	6.79	7.15
11	0.503	35	10.92	43.18	95	13.11		450	6.28	6.52
12	0.851	40	11.84	38.69	100	12.98	19.53	500	5.85	6.00
13	1.247	45	12.48	35.22	110	12.69	18.27	600	5.15	5.17
14	1.749	50	12.92	32.44	120	12.39	17.18	700	4.61	4.55
15	2.33	55	13.20		140	11.78	15.42	800	4.17	4.07
16	2.95	60	13.38	28.24	160	11.18	14.04	900	3.82	3.69
17	3.60	65	13.47		180	10.63	12.92	1000	3.53	3.37
18	4.24	70	13.50	25.21	200	10.12	11.98	2000	2.03	1.916
19	4.85	75	13.47		250	9.01	10.20	2500	1.691	1.676
20	5.43	80	13.42	22.89	300	8.12	8.91	3000	1.453	1.586

a deep Ramsauer–Townsend–like (RT) minimum located near 1.6 eV. At energies below the RT minimum (of 37×10^{-20} m^2), the TCS increases rapidly with decreasing energy and reaches the value of 53×10^{-20} m^2 at 0.6–0.7 eV. Above 1.6 eV, the TCS curve has a very broad enhancement of the maximum value 69×10^{-20} m^2, centered close to 8.5 eV. On the low-energy slope of this enhancement, the TCS curve shows a narrow resonant maximum peaking near 3.4 eV. The amplitude of this local maximum above slower rising TCS background amounts to about 5×10^{-20} m^2. It is also worth noting a weak shoulder in the TCS energy function, located between 6 and 7.5 eV. Beyond 10 eV, the TCS steadily decreases with increasing impact energy down to about 15×10^{-20} m^2 at 300 eV; nevertheless, some very weak changes in the slope of the curve, spanned between 20 and 30 eV and within 60–120 eV, are discernible.

Because the TCS contains the overall information on the scattering processes, a definite explanation of the aforementioned TCS structures to particular scattering events, without any additional electron-scattering studies, is a difficult task. Due to lack of detailed investigations on the electron impact from the 2-methyl–1,3-butadiene molecule, including the vibrational excitation and/or dissociative attachment, we can only speculate on the origin of the observed TCS features, based on results for particular scattering channels available for molecules of similar structure.

The appearance of the TCS curve below 1.6 eV can be partly explained in terms of the direct long-range interaction between the incoming electron and the target molecule possessing a permanent electric-dipole moment and an electric-dipole polarizability. For such targets the electron-scattering cross section exhibits the increase towards thermal energies [45]. The broad TCS hump spanned between 4 and 20 eV, with a maximum around 8.5 eV, closely resembles that for other targets, among them 1,3-C_4H_6 (cf. Fig. 3). Calculations for C_4H_6 isomers [46] indicate that this broad structure is mainly related with the elastic scattering. Because at these energies some inelastic-scattering processes are allowed, the contribution from a number of weak inelastic components is also expected.

The narrow peak located around 3.4 eV, superimposed onto the broad enhancement, can be attributed to the resonant process [47] occurring when the impinging electron of the specific energy is attached to the 2-methyl–1,3-butadiene molecule yielding a temporary parent negative-ion state. The extra electron is accommodated on the π^* molecular orbital

TABLE III. Ionization (ICS) and elastic (ECS) cross sections calculated for electron impact on 1,3-butadiene molecules; in units of 10^{-20} m^2.

E (eV)	ICS	E (eV)	ICS	ECS	E (eV)	ICS	ECS	E (eV)	ICS	ECS
8.80	0									
9	0.0372	25	6.22	45.57	85	10.50		350	5.81	6.29
10	0.234	30	7.61	38.74	90	10.42	16.62	400	5.34	5.67
11	0.433	35	8.63	33.98	95	10.32		450	4.94	5.17
12	0.686	40	9.35	30.46	100	10.22	15.43	500	4.60	4.76
13	1.050	45	9.85	27.74	110	9.99	14.44	600	4.05	4.11
14	1.464	50	10.19	25.56	120	9.75	13.58	700	3.62	3.62
15	1.929	55	10.41		140	9.27	12.20	800	3.28	3.23
16	2.40	60	10.55	22.27	160	8.80	11.11	900	3.00	2.93
17	2.91	65	10.61		180	8.36	10.23	1000	2.77	2.68
18	3.40	70	10.63	19.89	200	7.96	9.49	2000	1.598	1.520
19	3.86	75	10.62		250	7.09	8.08	2500	1.330	1.328
20	4.32	80	10.57	18.07	300	6.38	7.06	3000	1.142	1.254

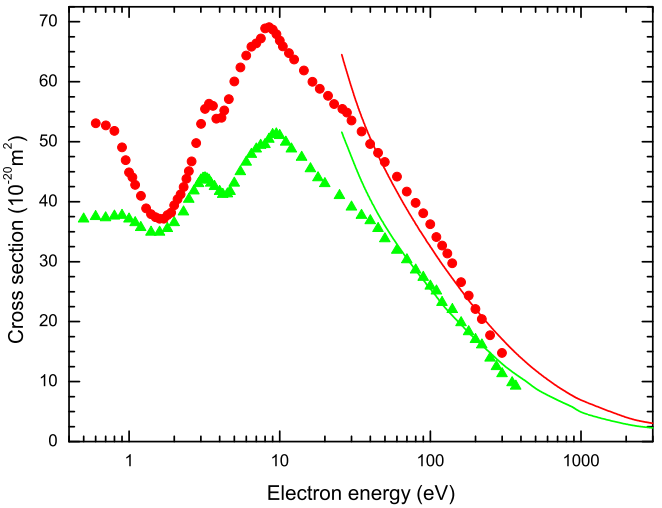

FIG. 3. Comparison of total absolute cross sections measured in our laboratory for electron scattering from molecules with conjugated double C=C bonds. 2-methyl–1,3-butadiene is shown by full (red) circles (present work). 1,3-butadiene is shown by full (green) triangles (from Ref. [10]). Also included are our computed (solid lines) cross sections, ECS + ICS, for respective molecules.

associated with the C=C double bonds. Support for such a statement is based on the observation that a similar structure has been noticed between 1.5 and 3 eV in the electron-scattering cross sections for other molecular targets, which (like the 2-methyl–1,3-butadiene molecule) have the C=C double bonds. For the ethylene ($H_2C = CH_2$) molecule, the simplest alkene, the formation of the π^* shape resonant state around 2 eV, due to the accommodation of the extra electron into the empty C=C π^* orbital, is now well established (cf. Ref. [48] and references therein). For more complex alkenes, the π^* resonant feature in the TCS energy curve, associated with the C=C bond, appears at slightly higher energies [10,49]. Figure 3 shows that the 1,3-butadiene molecule with two conjugated C=C bonds, the structural homologue of 2-methyl–1,3-butadiene (cf. Fig. 1), has a very similar TCS structure centered at 3.2 eV and attributed to the formation of a short-lived π^* parent anion [50,51].

The presence of the shoulder between 6 and 7.5 eV suggests that in this energy regime a resonant process can occur, which may lead to the vibrational excitation of the target molecule. This suggestion is based on fact that resonant structures in the excitation functions were observed within 5–9 eV for simpler hydrocarbons like C_2H_4 [48,52], C_2H_6 [53], C_3H_4 [54], and C_3H_6 [55]. The weak change in the slope of the TCS curve between 60 and 100 eV may be related to the ionization process, which is the most effective near 70–80 eV (see ICS curve in Fig. 2).

In Fig. 2 we also confront our experimental TCS values with the sum of computed integral ECS and ICS for 2-methyl–1,3-butadiene; the sum ECS + ICS represents here the theoretical estimate of the overall cross section. Between 25 and 300 eV, the general appearance of the ECS + ICS energy function looks similar to the measured TCS curve. Some disagreement in the magnitude of calculated total cross section and measurements, especially visible at lower impact energies, is associated with limitations of the AR model used for the computation of the elastic contribution to the scattering process. For a better estimate of the low-energy ECS curve, more sophisticated theoretical methods (e.g., see calculations for 1,3-butadiene in Ref. [46]) are necessary. Our calculations (Table II) indicate that, while at low-intermediate impact energies (see Fig. 2) the role of the elastic processes in the electron scattering is more dominant than the ionization, above 400 eV the contribution of both processes becomes comparable. Indeed, while around 100 eV the ECS amounts to about 60% of the sum of ECS and ICS, beyond 400 eV the contribution of ECS to the ECS + ICS oscillates between 49% and 51%.

B. Comparison of TCSs for electron scattering from 2-methyl–1,3-butadiene [C_5H_8] and 1,3-butadiene [C_4H_6] molecules: Effect of methylation

In this section, we examine how the methylation of hydrocarbon molecule; that is, the replacement of one hydrogen atom, bonded to carbon atom, with the methyl group [CH_3], affects the TCS energy dependence for the resulting compound. For this purpose, in Fig. 3 we compare our previous experimental TCS for 1,3-butadiene [H_2C=CHHC=CH_2] [10] to that currently obtained for its methylated homologue 2-methyl–1,3-butadiene [H_2C=C(CH_3)HC=CH_2] (for an illustration of the schematic geometry of these compounds see Fig. 1). We also compare calculated ECS + ICS values for both targets considered (see Tables II and III).

Figure 3 shows that, with respect to the overall shape, the TCS energy dependence for 2-methyl–1,3-butadiene resembles that for 1,3-butadiene. The TCS curves compared have two enhancements separated with the minimum located within 1.4–1.7 eV. However, the low-energy enhancement for the C_4H_6 compound is distinctly weaker than that for C_5H_8. This dissimilarity is associated with the difference between long-range contributions to the electron-molecule scattering for both considered targets. The replacement of one hydrogen atom in the 1,3-butadiene molecule with the CH_3 group leads to a change in the symmetry of charge-density distribution in the resultant compound. In effect, the 2-methyl–1,3-butadiene molecule has some permanent electric-dipole moment, while 1,3-C_4H_6 is a nonpolar (see Table IV). At energies above the minimum, both TCS energy functions have the narrow, resonant maximum centered at 3.2 eV for C_4H_6 and at 3.4 eV for the C_5H_8 molecule; it is evident that for the methylated molecule the resonant peak is less pronounced. The shift of the resonant TCS maximum towards higher energies caused by the consecutive methylation of molecule (increase of the number of methyl groups) has been recently demonstrated for series of methylated derivatives of ethylene [49] and acetylene [56]. This effect is related to the influence of the methyl unit on the electronic structure of the methylated compounds [57]. Close similarity in the behavior of both examined TCS curves concerns also a weak shoulder discernible around 7 eV. On the other hand, the main TCS maximum is located at different energies, near 9.5 eV for C_4H_6 and close to 8.5 eV for C_5H_8.

It is evident from Fig. 3 that the magnitude of TCS for 2-methyl–1,3-butadiene is distinctly higher than that for 1,3-butadiene. The larger TCS for 2-methyl–1,3-butadiene is

TABLE IV. Selected electric parameters for considered compounds (from Ref. [60]): the permanent dipole moment μ and the static dipole polarizability α. Location of the first resonant-like maximum E_{1max} observed in the TCS curves.

Molecule	E_{1max} (eV)	μ (Debye)	α (10^{-30}m^3)
$H_2C{=}C(CH_3){-}HC{=}CH_2$; 2-methyl–1,3-butadiene	3.4[a]	0.25	9.99
$H_2C{=}CH{-}HC{=}CH_2$; 1,3-butadiene	3.2[b]	0	8.64

[a]Present work.
[b]Reference [10].

associated with the increase of its molecular size due to the presence of the extra methyl unit. The ratio $TCS(C_5H_8)/TCS(C_4H_6)$ is nearly constant (1.3–1.4) over almost the entire energy range investigated. However, the role of methylation seems to decrease in the vicinity of the TCS minimum, between 1 and 2.5 eV, where this ratio does not exceed 1.1–1.2. Further analysis of TCS results reveals that the difference in the magnitude of TCS for both targets, at given impact energy E, appears to be nearly equal to half of $TCS(E)$ for the ethane [C_2H_6] molecule (from Ref. [11]); that means the $0.5 \times TCS(C_2H_6)$ may represent the TCS for the methyl unit, CH_3. Figure 4 shows that the TCS for 2-methyl–1,3-butadiene obtained as sum of TCS for 1,3-butadiene and half of that for the ethane molecule is in a good agreement with the current experimental TCS data, especially for energies above 5 eV. The disaccord estimated that way and the measured TCSs for 2-methyl–1,3-butadiene at lower impact energies is associated with the fact that the simple addition of TCSs for constituents does not take into account a change of the charge-density distribution after methylation. Based on the above-mentioned finding we have estimated TCS for 2,3-dimethyl–1,3-butadiene, C_6H_{12}, [$H_2C{=}CH(CH_3)(CH_3)HC{=}CH_2$] molecule (see Fig. 4), the next member of this family.

To check how the methylation of targets of different molecular structure is reflected in their TCS energy function, we also examine the TCS results for allenes (allene [$H_2C{=}C{=}CH_2$], from Ref. [58]; 1,2-butadiene [$H_2C{=}C{=}CH(CH_3)$], from Ref. [59]) and for acetylenes (acetylene [$HC{\equiv}CH$]; propyne [$HC{\equiv}C(CH_3)$], and 2-butyne [$(CH_3)C{\equiv}C(CH_3)$], from Refs. [10,49,58]). We found, that for both molecular families, at a given impact energy, the magnitude of the TCS for every subsequent methyl-substituted molecule in series is higher than that of previous one by almost the same value. The difference in the magnitude appears to be nearly equal to one half of TCS for the ethane molecule at each corresponding energy, just as for the 1,3-butadiene series.

Figure 5 shows experimental TCSs for allene, a molecule having two C=C double bonds sharing a common carbon atom, and its methylated derivative 1,2-butadiene. Depicted is also the TCS for 1,2-butadiene estimated by the additivity

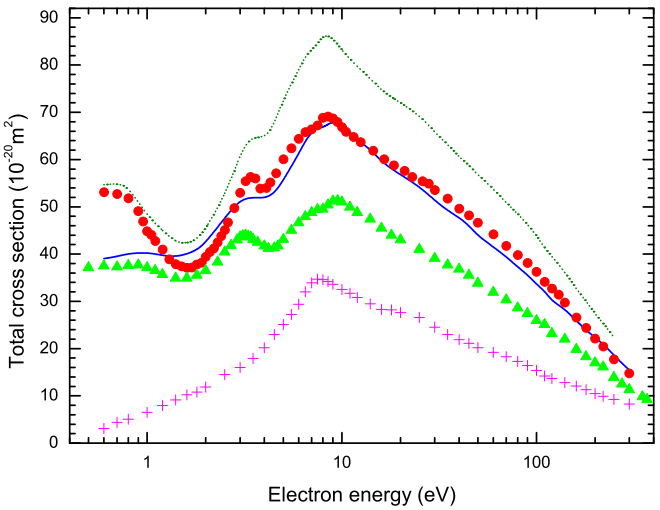

FIG. 4. Illustration of how the TCS measured for the 2-methyl–1,3-butadiene molecule can be reproduced by a sum of the TCS for 1,3-butadiene and half of the TCS for the ethane molecule. 2-methyl–1,3-butadiene is shown by full (blue) line (estimated TCS). Full (red) circles show experimental TCS (present work). 1,3-butadiene is shown by full (green) triangles (experimental TCS, from Ref. [10]). Ethane is shown by crosses (magenta) (experimental TCS, from Ref. [11]). The dot-dot (olive) line shows the TCS curve predicted for 2,3-dimethyl–1,3-butadiene.

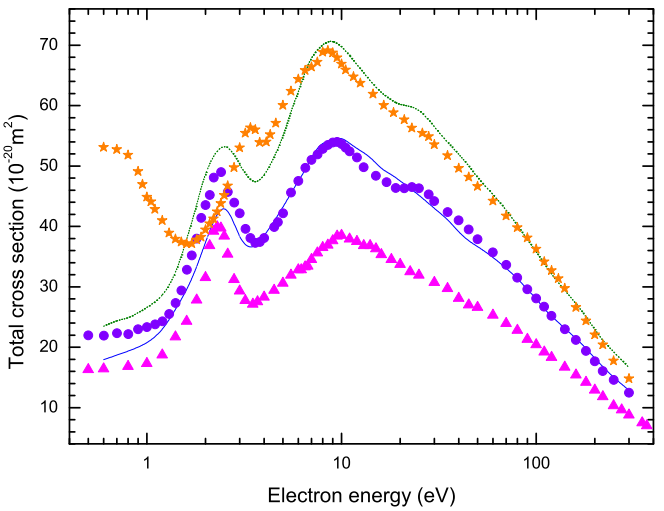

FIG. 5. Illustration of the role of methylation in the electron scattering from allenes. Allene, full (magenta) triangles, experimental TCS, from Ref. [58]. 1,2-butadiene: full (violet) circles, experimental TCS, from Ref. [59]. Full (blue) line shows the estimate by the sum of the TCS for allene [58] and half of the TCS for the ethane molecule (see Fig. 4). Depicted also is TCS for 3-methyl–1,2-butadiene [dot-dot (dark yellow) line], the estimate by the sum of the TCS for 1,2-butadiene and half of the TCS for ethane. The present experimental TCS for 2-methyl–1,3-butadiene molecule (isomer of 3-methyl–1,2-butadiene) is shown by full (orange) stars.

procedure: TCS(allene) + 0.5 × TCS(ethane). The agreement of the experimental and estimated TCSs is very good. Figure 5 also shows that the TCS for 3-methyl–1,2-butadiene [$H_2C{=}C{=}C(CH_3)_2$], estimated the same way, is in a good accord with the present experimental TCS data for its isomer, 2-methyl–1,3-butadiene. Because isomeric molecules have similar TCSs beyond 30–50 eV, such an agreement confirms that TCS values estimated this way for the 3-methyl–1,2-butadiene molecule are reliable.

V. SUMMARY

We present herein our experimental and theoretical cross sections for electron scattering by the 2-methyl–1,3-butadiene molecule. To examine how the methylation affects the shape and/or magnitude of the cross-section energy function, we compared these results with our previous results for the 1,3-butadiene [C_4H_6] molecule. With respect to the shape, there is a close similarity between the present measured TCS curve for 2-methyl–1,3-butadiene and the TCS for its structural homologue 1,3-butadiene [10]. However, the characteristic TCS features (maxima and minimums) for 2-methyl–1,3-butadiene are shifted in energy by about 0.2–1 eV with respect to those in 1,3-butadiene. The presence of the extra methyl group in 2-methyl–1,3-butadiene reflects mainly in general increase of the TCS magnitude for this compound. We also find that the experimental TCS for 2-methyl–1,3-butadiene can be obtained with a quite good approximation as the sum of the TCS for 1,3-butadiene and the TCS for the methyl unit, which is estimated as half of the TCS for the ethane molecule. Similar regularity was noticed for other series of methylated targets. That regularity enables the reasonable TCS estimate for members of methyl-substituted families.

ACKNOWLEDGMENTS

This work has been partially supported by the Polish Ministry of Science and Higher Education [MNiSzW (Poland) Project 2015-2016]. This work was conducted within the framework of the COST (Eur. Union) Action CM1301 (CELINA). Numerical calculations were performed at the Academic Computer Center (TASK) in Gdańsk.

[1] N. J. Mason, J. Phys.: Conf. Ser. **565**, 012201 (2014).
[2] L. Sanche, Nature (London) **461**, 358 (2009); Chem. Phys. Lett. **474**, 1 (2009).
[3] M. Fuss, A. Muñoz, J. C. Oller, F. Blanco, P. Limão-Vieira, C. Huerga, M. Téllez, M. J. Hubin-Franskin, K. Nixon, M. Brunger, and G. García, J. Phys.: Conf. Ser. **194**, 012028 (2009).
[4] F. Blanco, A. Muñoz, D. Almeida, F. Ferreira da Silva, P. Limão-Vieira, M. C. Fuss, A. G. Sanz, and G. García, Eur. Phys. J. D **67**, 199 (2013).
[5] Y. Itikawa, *Molecular Processes in Plasmas* (Springer, Berlin, Heidelberg, New York, 2007).
[6] L. G. Christophorou and J. K. Olthoff, *Fundamental Electron Interactions with Plasma Processing Gases* (Kluwer Academic/Plenum Publishers, New York, 2004).
[7] S. Engman, M. Stano, S. Matejčik, and O. Ingólfsson, Phys. Chem. Chem. Phys. **14**, 14611 (2012).
[8] E. Böhler, J. Warneke, and P. Swiderek, Chem. Soc. Rev. **42**, 9219 (2013).
[9] R. M. Thorman, T. P. Ragesh Kumar, H. Fairbrother, and O. Ingólfsson, Beilstein J. Nanotechnol. **6**, 1904 (2015).
[10] Cz. Szmytkowski and S. Kwitnewski, J. Phys. B: At., Mol. Opt. Phys. **36**, 2129 (2003).
[11] Cz. Szmytkowski and A. Krzysztofowicz, J. Phys. B: At., Mol. Opt. Phys. **28**, 4291 (1995).
[12] T. D. Sharkey, A. E. Wiberley, and A. R. Donohue, Ann. Botany **101**, 5 (2008), and references therein.
[13] R. Salerno-Kennedy and K. D. Cashman, Wien. Klin. Wochenschr. **117**, 180 (2005).
[14] J. D. Morrison and A. J. C. Nicholson, J. Chem. Phys. **20**, 1021 (1952).
[15] P. R. C. Lopes, A. B. Guenther, A. A. Turnipseed, D. Bonal, D. Serça, B. Burban, L. Siebicke, L. Emmons, and J. O. W. V. Bustillos, in *Proceedings of International Nuclear Atlantic Conference INAC 2013* (Associação, Recife, Brazil, 2013), https://www.ipen.br/biblioteca/2013/inac/19299.pdf.
[16] G. Martins, A. M. Ferreira-Rodrigues, F. N. Rodrigues, G. G. B. de Souza, N. J. Mason, S. Eden, D. Duflot, J.-P. Flament, S. V. Hoffmann, J. Delwiche, M. J. Hubin-Franskin, and P. Limão-Vieira, Phys. Chem. Chem. Phys. **11**, 11219 (2009).
[17] L. V. Vilkov and N. I. Sadova, J. Struct. Chem. **8**, 353 (1968).
[18] Cz. Szmytkowski, P. Możejko, and G. Kasperski, J. Phys. B **30**, 4363 (1997); Cz. Szmytkowski and P. Możejko, Vacuum **63**, 549 (2001); A. Domaracka, P. Możejko, E. Ptasińska-Denga, and Cz. Szmytkowski, J. Phys. B **39**, 4289 (2006).
[19] R. E. Kennerly, Phys. Rev. A **21**, 1876 (1980).
[20] Cz. Szmytkowski, K. Maciąg, and G. Karwasz, Phys. Scr. **54**, 271 (1996).
[21] M. Knudsen, Ann. Phys. Lpz. **336**, 633 (1910).
[22] G. G. Raju, *Gaseous Electronics: Tables, Atoms, and Molecules* (CRC Press, Boca Raton, 2011).
[23] B. Bederson and L. J. Kieffer, Rev. Mod. Phys. **43**, 601 (1971).
[24] J. P. Sullivan, J. Makochekanva, A. Jones, P. Caradonna, D. S. Slaughter, J. Machacek, R. P. McEachran, D. W. Mueller, and S. J. Buckman, J. Phys. B: At., Mol. Opt. Phys. **44**, 035201 (2011).
[25] R. N. Nelson and S. O. Colgate, Phys. Rev. A **8**, 3045 (1973).
[26] N. F. Mott and H. S. W. Massey, *The Theory of Atomic Collisions* (Oxford University Press, Oxford, 1965).
[27] Y.-K. Kim and M. E. Rudd, Phys. Rev. A **50**, 3954 (1994); W. Hwang, Y.-K. Kim, and M. E. Rudd, J. Chem. Phys. **104**, 2956 (1996).
[28] P. Możejko, B. Żywicka-Możejko, and Cz. Szmytkowski, Nucl. Instrum. Methods Phys. Res., Sect. B **196**, 245 (2002).
[29] F. Salvat, J. D. Martinez, R. Mayol, and J. Parellada, Phys. Rev. A **36**, 467 (1987).
[30] N. T. Padial and D. W. Norcross, Phys. Rev. A **29**, 1742 (1984).
[31] J. P. Perdew and A. Zunger, Phys. Rev. B **23**, 5048 (1981).
[32] X. Zhang, J. Sun, and Y. Liu, J. Phys. B: At., Mol. Opt. Phys. **25**, 1893 (1992).
[33] M. J. Frisch, G. W. Trucks, H. B. Schlegel, G. E. Scuseria, M. A. Robb, J. R. Cheeseman, G. Scalmani, V. Barone, B. Mennucci, G. A. Petersson, H. Nakatsuji, M. Caricato, X. Li,

H. P. Hratchian, A. F. Izmaylov, J. Bloino, G. Zheng, J. L. Sonnenberg, M. Hada, M. Ehara, K. Toyota, R. Fukuda, J. Hasegawa, M. Ishida, T. Nakajima, Y. Honda, O. Kitao, H. Nakai, T. Vreven, J. A. Montgomery, Jr., J. E. Peralta, F. Ogliaro, M. Bearpark, J. J. Heyd, E. Brothers, K. N. Kudin, V. N. Staroverov, T. Keith, R. Kobayashi, J. Normand, K. Raghavachari, A. Rendell, J. C. Burant, S. S. Iyengar, J. Tomasi, M. Cossi, N. Rega, J. M. Millam, M. Klene, J. E. Knox, J. B. Cross, V. Bakken, C. Adamo, J. Jaramillo, R. Gomperts, R. E. Stratmann, O. Yazyev, A. J. Austin, R. Cammi, C. Pomelli, J. W. Ochterski, R. L. Martin, K. Morokuma, V. G. Zakrzewski, G. A. Voth, P. Salvador, J. J. Dannenberg, S. Dapprich, A. D. Daniels, O. Farkas, J. B. Foresman, J. V. Ortiz, J. Cioslowski, and D. J. Fox, GAUSSIAN 09, Revision D.01 (Wallingford, Gaussian, Inc., 2013).

[34] L. S. Cederbaum, J. Phys. B: At. Mol. Phys. **8**, 601 (1975).

[35] W. von Niessen, J. Schirmer, and L. S. Cederbaum, Comput. Phys. Rep. **1**, 57 (1984).

[36] J. V. Ortiz, J. Chem. Phys. **89**, 6348 (1988).

[37] V. G. Zakrzewski and W. von Niessen, J. Comput. Chem. **14**, 13 (1994).

[38] Cz. Szmytkowski, P. Możejko, S. Kwitnewski, E. Ptasińska-Denga, and A. Domaracka, J. Phys. B: At., Mol. Opt. Phys. **38**, 2945 (2005).

[39] P. Możejko, E. Ptasińska-Denga, A. Domaracka, and Cz. Szmytkowski, Phys. Rev. A **74**, 012708 (2006).

[40] P. Możejko, A. Domaracka, E. Ptasińska-Denga, and Cz. Szmytkowski, Chem. Phys. Lett. **429**, 378 (2006).

[41] Cz. Szmytkowski, P. Możejko, S. Kwitnewski, A. Domaracka, and E. Ptasińska-Denga, J. Phys. B: At., Mol. Opt. Phys. **39**, 2571 (2006).

[42] Cz. Szmytkowski, A. Domaracka, P. Możejko, and E. Ptasińska-Denga, Phys. Rev. A **75**, 052721 (2007).

[43] Cz. Szmytkowski, P. Możejko, E. Ptasińska-Denga, and A. Sabisz, Phys. Rev. A **82**, 032701 (2010).

[44] P. Możejko, E. Ptasińska-Denga, and Cz. Szmytkowski, Eur. Phys. J. D **66**, 44 (2012).

[45] Y. Itikawa, Int. Rev. Phys. Chem. **16**, 155 (1997).

[46] A. R. Lopes, M. A. P. Lima, L. G. Ferreira, and M. H. F. Bettega, Phys. Rev. A **69**, 014702 (2004).

[47] K. Takayanagi, in *Electron-Molecule Collisions*, edited by I. Shimamura and K. Takayanagi (Plenum Press, New York, London, 1984).

[48] M. A. Khakoo, S. M. Khakoo, A. Sakaamini, B. A. Hlousek, L. R. Hargreaves, J. Lee, and R. Murase, Phys. Rev. A **93**, 012710 (2016).

[49] Cz. Szmytkowski, S. Stefanowska, M. Zawadzki, E. Ptasińska-Denga, and P. Możejko, J. Chem. Phys. **143**, 064306 (2015).

[50] P. D. Burrow and K. D. Jordan, Chem. Phys. Lett. **36**, 594 (1975).

[51] J. Rutkowsky, H. Drost, and H.-J. Spangenberg, Ann. Phys. (Berlin, Ger.) **37**, 259 (1980).

[52] I. C. Walker, A. Stamatovic, and S. F. Wong, J. Chem. Phys. **78**, 5532 (1978); M. Allan, C. Winstead, and V. McKoy, Phys. Rev. A **77**, 042715 (2008).

[53] L. Boesten, H. Tanaka, M. Kubo, H. Sato, M. Kimura, M. A. Dillon, and D. Spence, J. Phys. B **23**, 1905 (1990); R. Merz and F. Linder, *ibid.* **36**, 1143 (2003).

[54] Y. Nakano, M. Hoshino, M. Kitajima, H. Tanaka, and M. Kimura, Phys. Rev. A **66**, 032714 (2002).

[55] M. Allan and L. Andric, J. Chem. Phys. **105**, 3559 (1996); R. Čurik, P. Čársky, and M. Allan, Phys. Rev. A **86**, 062709 (2012).

[56] Cz. Szmytkowski, P. Możejko, M. Zawadzki, K. Maciąg, and E. Ptasińska-Denga, Phys. Rev. A **89**, 052702 (2014).

[57] L. Libit and R. Hoffmann, J. Am. Chem. Soc. **97**, 1370 (1974).

[58] Cz. Szmytkowski and S. Kwitnewski, J. Phys. B: At., Mol. Opt. Phys. **35**, 3781 (2002).

[59] Cz. Szmytkowski, P. Możejko, M. Zawadzki, and E. Ptasińska-Denga, J. Phys. B **48**, 025201 (2015).

[60] D. R. Lide (ed.), in *Handbook of Chemistry and Physics*, 76th ed. (CRC Press, Boca Raton, 1995–1996).